

First-order transition from ferromagnetism to antiferromagnetism in $\text{Ce}(\text{Fe}_{0.96}\text{Al}_{0.04})_2$: A magnetotransport study

Kanwal Jeet Singh, Sujeet Chaudhary,* M. K. Chattopadhyay, M. A. Manekar, S. B. Roy, and P. Chaddah
Low Temperature Physics Laboratory, Centre for Advanced Technology, Indore 452 013, India

(Received 23 August 2001; revised manuscript received 4 October 2001; published 13 February 2002)

Magnetotransport behavior is investigated in detail across a first-order magnetic phase transition from a ferromagnetic state to an antiferromagnetic state in a polycrystalline $\text{Ce}(\text{Fe}_{0.96}\text{Al}_{0.04})_2$ sample. The study clearly brings out various generic features associated with a first-order transition, viz., hysteresis, phase coexistence, supercooling and superheating, and the presence and limits of the metastable regimes. These magnetotransport study results exhibit and support all the interesting thermomagnetic history effects that were observed in our earlier dc magnetization study on the same sample. Most notable here is the initial (or virgin) resistivity vs field curve lying outside the hysteretic “butterfly-shaped” magnetoresistivity loops obtained on cycling the magnetic field between high enough positive and negative strengths. These findings, bearing a one-to-one similarity with the data obtained in their magnetic counterpart (i.e., dc magnetization), are ascribed an origin due to the arresting of this first-order transition kinetics at low temperature and high magnetic field.

DOI: 10.1103/PhysRevB.65.094419

PACS number(s): 75.30.Kz, 64.60.My, 75.60.-d, 75.90.+w

I. INTRODUCTION

The C15-Laves phase CeFe_2 compound, which crystallizes in the form of a cubic MgCu_2 -type structure, is an unstable ferromagnet with a Curie temperature $T_C \approx 235$ K. Upon doping with small concentrations of metals like Co, Ru, Ir, Al, Os, Re, etc., at the Fe site, the ferromagnetic (FM) behavior disappears at low temperature, and the pseudobinary system $\text{Ce}(\text{Fe}_{1-x}\text{R}_x)_2$ exhibits a stable antiferromagnetic (AFM) phase¹⁻¹¹ below a certain temperature which we shall henceforth refer to as T_N . There exists an extensive amount of research work on this interesting magnetic system. Various experimental tools have been employed to ascertain the true magnetic state of a Ce sublattice and the instabilities related to an Fe sublattice. Studies based on neutron scattering,¹²⁻¹⁴ magnetic circular x-ray dichroism,¹⁵⁻¹⁷ magneto-optic Kerr effect,¹⁸ high-energy spectroscopy (including x-ray photoemission, absorption, ultraviolet),^{19,20} magnetic Compton scattering,²¹ specific heat,²² magnetization,^{8-11,23,24} magnetotransport,²⁵⁻²⁸ ac susceptibility,²⁹⁻³² etc. were reported in pure and doped CeFe_2 alloys. While these studies were mainly associated with the understanding of the magnetic instability in $\text{Ce}(\text{Fe}_{1-x}\text{R}_x)_2$, we have recently started probing the exact nature of the magnetic phase transition (AFM to FM), which can be driven by high enough magnetic field (H) even at temperatures (T) much below $T_N \approx 100$ K. Our preliminary attempt on this front started initially with an ac susceptibility study³³ and an investigation of the dc magnetization behavior³⁴ in Ru- and Ir-doped CeFe_2 alloys, namely, polycrystalline $\text{Ce}(\text{Fe}_{0.95}\text{Ir}_{0.05})_2$ and $\text{Ce}(\text{Fe}_{0.93}\text{Ru}_{0.07})_2$ samples. In these studies (based primarily on arguments of hysteresis and phase coexistence) the AFM-to-FM transition is found to be of first order in nature. Due to the very narrow hysteretic regime in these Ru- and Ir-doped CeFe_2 alloys, we decided to investigate the $\text{Ce}(\text{Fe}_{0.96}\text{Al}_{0.04})_2$ alloy wherein the AFM-to-FM transition is relatively gradual;^{6,7} this sample also provided us with a distinctly wider H - T phase space [permitted

by the maximum magnetic field (i.e., 5.5 T) in our superconducting quantum interference device magnetometer] for a more comprehensive study of the nature of magnetic transition in this system. This revealed a further interesting dc magnetization behavior^{35,36} which along with some of our preliminary results for magnetotransport measurements,³⁶ led us to clearly establish the first-order nature of the AFM-to-FM transition in the $\text{Ce}(\text{Fe}_{0.96}\text{Al}_{0.04})_2$ alloy. The present paper deals with our detailed magnetotransport study on the same sample used in Refs. 35 and 36. Although preliminary results of a magnetotransport study on $\text{Ce}(\text{Fe}_{0.96}\text{Al}_{0.04})_2$ were published in Ref. 36, in this paper we (i) extend our investigation regime in the the resistivity ρ vs T hysteresis data to higher H ; (ii) present ρ vs H hysteresis data to lower T ; (iii) measure minor hysteresis loops in ρ vs T ; (iv) compare ρ vs T data obtained in zero-field cooled and field-cooled cooling histories with that recorded during field-cooled warming of the sample; and (v) study ρ by following a more contrived history dependence of the external magnetic field. The present work shows that the $\text{Ce}(\text{Fe}_{0.96}\text{Al}_{0.04})_2$ compound can be taken as a model system where one can observe most of the generic features related with a first-order phase transition. We interpret all these results in the light of a first-order transition and its associated behavior (e.g., hysteresis, phase coexistence, supercooling and superheating, and a field-dependent thermomagnetic history of magnetotransport behavior). In addition, a comparison of the present work on $\text{Ce}(\text{Fe}_{0.96}\text{Al}_{0.04})_2$ alloy is being made with the existing work on perovskite-type manganese oxide compounds³⁷⁻³⁹ at appropriate places.

II. EXPERIMENT

The $\text{Ce}(\text{Fe}_{0.96}\text{Al}_{0.04})_2$ alloy sample employed in the present magnetotransport study belongs to the same batch of samples used earlier in the study of bulk magnetic and transport properties⁶ and neutron measurements.¹² Details of the sample preparation and characterization can be found in Ref. 6. A commercial cryostat (Oxford Instruments Inc., UK) with

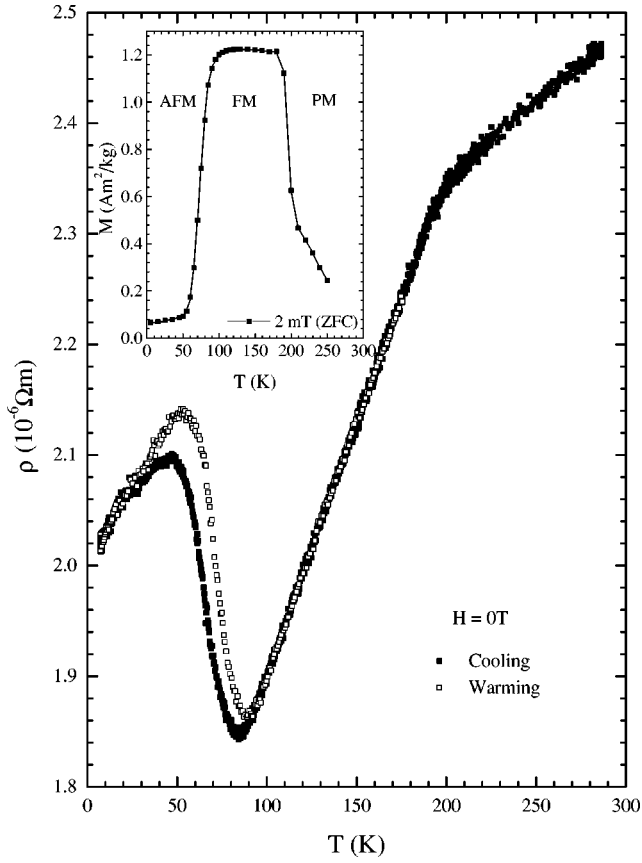


FIG. 1. Resistivity vs temperature plot for a $\text{Ce}(\text{Fe}_{0.96}\text{Al}_{0.04})_2$ sample recorded during the initial cooling (filled square symbols) from above 290 K to 4.5 K, and subsequent warming cycle (open square symbols). The inset shows a temperature dependence of dc magnetization on the same sample recorded in a field of 2.0 mT.

a maximum magnetic field of 16 T, was used for carrying out the four-probe resistivity measurement as a function of temperature and magnetic field H applied transverse to the measuring current. The isofield ρ vs T data were recorded with the following different protocols.

(1) Zero-field cooling (ZFC): The sample was first cooled from above T_C down to lowest temperature of measurement in zero field, then subjected to a magnetic field, and $\rho(T)$ data were recorded during warming of the sample.

(2) Field-cooled cooling (FCC): The sample was subjected to the desired magnetic-field strength above its T_C , and the $\rho(T)$ data were recorded while cooling the sample.

(3) Field-cooled warming (FCW): The resistivity of the sample was measured as a function of T during warming of the sample which was earlier field cooled to the lowest investigated temperature.

III. RESULTS

Figure 1 shows the T dependence of the resistivity for the $\text{Ce}(\text{Fe}_{0.96}\text{Al}_{0.04})_2$ sample in the absence of magnetic field, recorded during the initial cooling cycle starting from 290 K as well as during the subsequent warming cycle. During the initial decrease in the temperature, while the paramagnetic (PM) to FM transition is reflected in the change of slope in

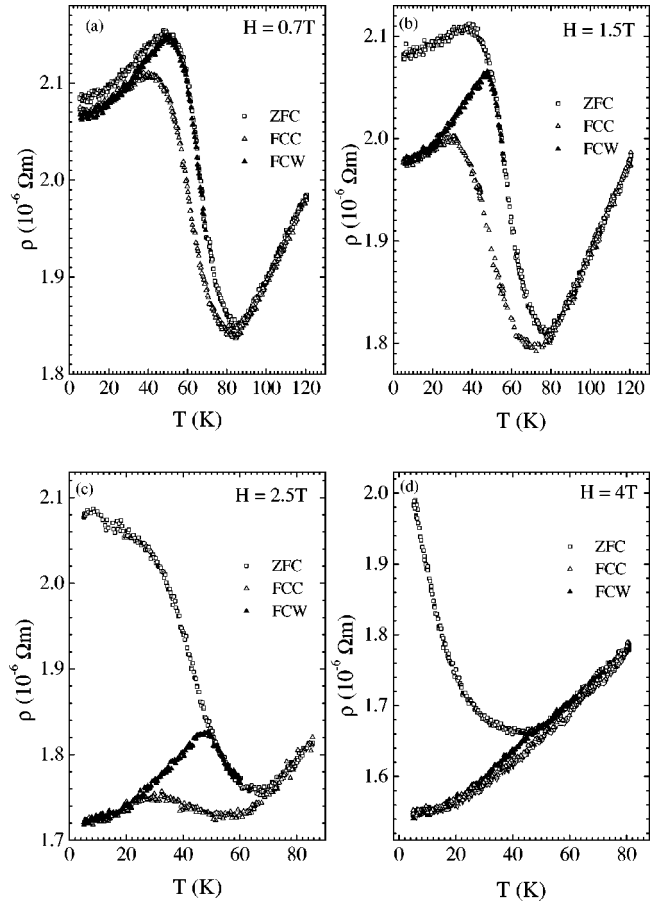


FIG. 2. Effect of magnetic field on the ρ vs T plots for a $\text{Ce}(\text{Fe}_{0.96}\text{Al}_{0.04})_2$ sample recorded under different measurement protocols, viz. ZFC (open square symbols), FCC (open triangle symbols) and FCW (filled triangle symbols): (a) 0.7 T, (b) 1.5 T, (c) 2.5 T, and (d) 4.0 T.

the ρ vs T plot at about 200 K, the rise of ρ is observed below about 84 K due to a second magnetic phase transition from FM- to AFM-ordered states. This second transition is completed at about 35 K (while cooling), below which the resistivity once again decreases with a decrease in temperature. For comparison, in the inset of Fig. 1 we present a dc magnetization M vs T plot for the same sample in a 2-mT magnetic field. The three magnetic phases marked as PM, FM, and AFM in different T regimes complement our present results for the resistivity measurement. During the thermal cycling (i.e., warming and cooling), the resistivity behavior exhibited a distinct hysteresis across the FM-to-AFM transition (see the main panel of Fig. 1).

In Figs. 2(a)–2(d), ρ vs T plots for magnetic-field strengths of 0.7, 1.5, 2.5, and 4.0 T, respectively, are shown for the three different histories of application of magnetic field, e.g., ZFC, FCC, and FCW (ρ vs T plots in ZFC and FCC protocols for other fields; 0.5, 2.0, and 3.0 T can be found in Fig. 4 of Ref. 36). As is evident from Figs. 2(a)–2(d), the resistivity plots for all three protocols—ZFC, FCC, and FCW—are strongly affected by the strength of the applied magnetic field across the FM-AFM transition. Note that both the onset and completion of AFM-FM transitions are

shifted to lower temperatures in the presence of a magnetic field. This shift is again found to be strongly field dependent. Compared to a value of ≈ 93 K for the completion of the AFM-FM transition while warming the sample in the absence of field (see Fig. 1), the same transition is completed only by ≈ 46 K when a magnetic field of 4 T is applied [see Fig. 2(d)]. The magnetic field has another interesting effect in the low-temperature AFM state. Above a certain value of H (i.e., 0.5 T), the FCC resistivity stays below the ZFC resistivity at low temperatures (also see Fig. 4 of Ref. 36). At any temperature, this difference of resistivity is field dependent, increasing with the applied magnetic field. Furthermore, starting at 4.5 K, the FCW data overlap with the FCC data up to some field-dependent temperature. Above this temperature, the FCW curve continues to rise (in contrast to the falling FCC curve), until it merges with the ZFC curve at some slightly higher T . Thus the ρ vs T curves under the FCC and FCW protocols show a downturn at different temperatures. It should be noted here that above the merger point of FCW and ZFC- $\rho(T)$ curves, the $\rho(T)$ curve of the FCC protocol lies distinctly below that recorded in the FCW protocol. We stress here that the FCW protocol is basically a minor hysteresis loop of the second kind (as described in the next paragraph) initiated from the lowest investigated temperature.

Figure 3 shows the results obtained across what are called the “minor hysteresis loops” (MHL’s) in the absence of external magnetic field. Two kinds of MHL’s are recorded. In the first kind, the sample is initially warmed from sufficiently low temperatures, and then from a predetermined temperature the sample is cooled back. The MHL initiated at 44.5 K from the warming cycle (Fig. 3) is an example of this kind. In the second kind, the sample is initially cooled (from well above T_C) up to a predetermined temperature, and then is warmed. The MHL’s initiated on the cooling curve at 60, 75, and 84 K in Fig. 3 are examples of this kind. It can be clearly seen that the two MHL’s initiated near the onset and completion of the AFM-FM transition, respectively at 44.5 and 84 K are reversible. However, the MHL’s initiated from the cooling curve at 60 and 75 K followed an altogether different path. They finally merged with the warming curve (initiated from 4.5 K, and were henceforth referred to as envelope warming curve).

The isothermal ρ vs H data were also recorded at various temperatures ranging from 2 to 120 K. In Figs. 4(a) and 4(b), we show the ρ vs H data for the lowest temperature (i.e., 2 K) and at 100 K, respectively. Within our accuracy of measurements, the ρ vs H plots for $T \geq 100$ K were found to be linear right from 0 T. As pointed out previously,³⁶ the $\rho(H)$ behavior at lower temperatures is quite interesting. A small rise in ρ with initial increase of H (within the AFM regime) along the virgin curve is observed only at 2 K [see Fig. 4(a)].

Finally, in Fig. 5 we present the results of resistivity measurements in a 0.7-T magnetic field during a warming cycle starting from a 4.5-K temperature point, which is approached using an altogether different protocol. In this protocol, the final state (i.e., 4.5 K and 0.7 T) is prepared following two steps. The first step involved the FCC protocol in 2.5 T from above T_C to 4.5 K. Subsequent to this, in a second step, the

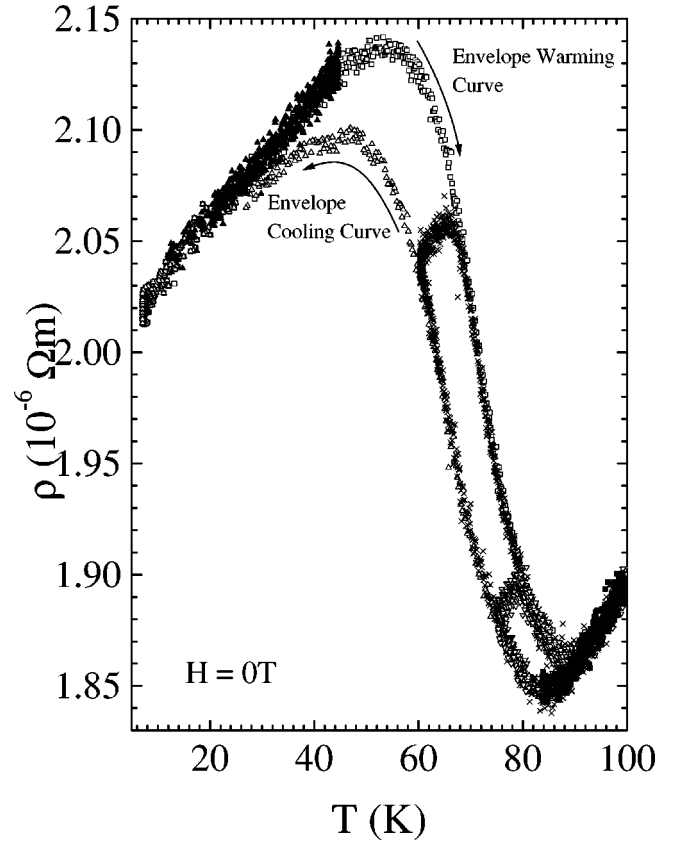


FIG. 3. The minor hysteresis loops for a $\text{Ce}(\text{Fe}_{0.96}\text{Al}_{0.04})_2$ sample initiated from the envelope warming curve (open square symbols) at 44.5 K (filled up-triangle symbols), and from the envelope cooling curve (open up-triangle symbols) at 60 K (cross symbols), 75 K (open down-triangle symbols), and 84 K (filled square symbols). Refer to the text for more details.

field was reduced isothermally from 2.5 to 0.7 T (these two steps are indicated as path I in the inset of Fig. 5). For the purpose of comparison, the $\rho(T)$ plots for FCC and FCW protocols at 0.7 T (corresponding to cooling and warming along the path II, as indicated in the inset of Fig. 5) are also shown in Fig. 5. With the initial reduction of field from a 2.5- to a 0.7-T field at 4.5 K, the resistivity value showed a jump (as indicated by a vertical arrow from point marked A at 4.5 K in Fig. 5) to a value (marked as point B in Fig. 5) which was smaller than the $\rho(4.5 \text{ K}, 0.7 \text{ T})$ value recorded in any of the conventional ZFC, FCC, or FCW measurement protocols for $H = 0.7$ T. However, upon a subsequent warming of the sample, the resistivity was found to increase as shown in Fig. 5, until it finally merged with the ρ vs T curve at 0.7 T, corresponding to the FCW protocol.

IV. DISCUSSION

A. First-order AFM-to-FM transition and the associated hysteresis

Based on the ρ vs T data, we first argue that with increase in temperature and/or field, the low-temperature low-field AFM phase transforms to a FM phase through a first-order transition (FOT). The first indication of a FOT comes in the

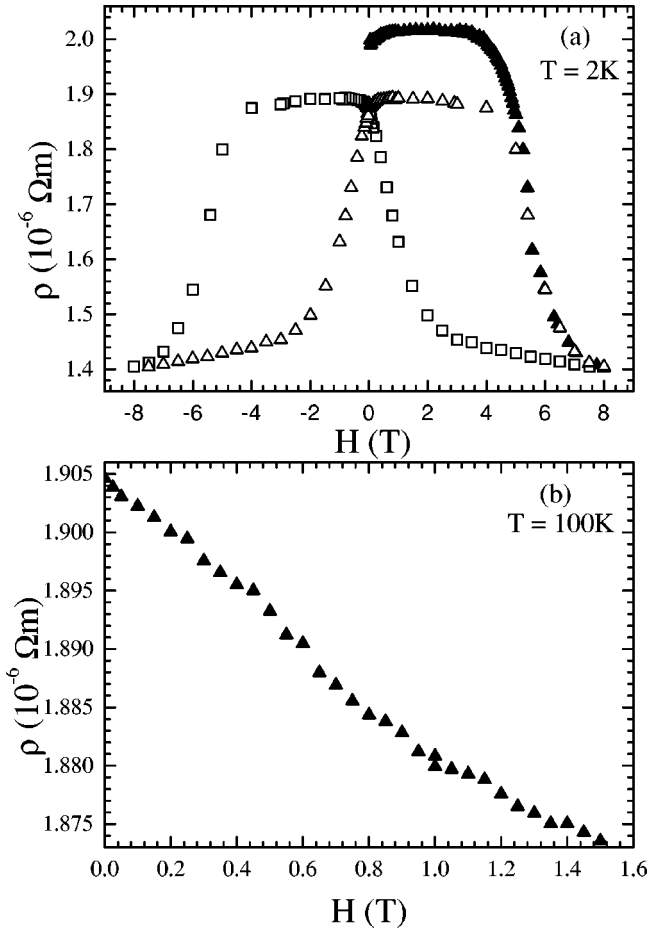


FIG. 4. The isothermal ρ vs H plots for a $\text{Ce}(\text{Fe}_{0.96}\text{Al}_{0.04})_2$ sample recorded at (a) 2 K and (b) 100 K. The three different histories of H and T in the ρ vs T behavior (at 2 K), i.e., the virgin resistivity curve (starting from $H=0$ after initially cooling the sample to the desired temperature in zero field), the envelope H -decreasing resistivity curve, and the envelope H -increasing resistivity curve are shown by the filled triangle, the open square, and the open triangle, respectively. See the text for details.

form of a hysteresis in the resistivity, which is observed at both temperature (Figs. 1 and 2) and field cyclings [Fig. 4(a)]. During the cooling of the sample, the onset of the rise of resistivity starts with the nucleation of the AFM phase at ≈ 84 K (Fig. 1). This upturn in resistivity basically occurs due to the appearance of magnetic superzones at the onset of the FM-AFM transition^{6,7} (i.e., at T_N). Further cooling converts more and more of the sample from a FM state to an AFM state, with the result that the entire sample transforms into an AFM state below about 35 K. During the warming cycle, the decrease in resistivity at the transition is slightly delayed compared to the cooling cycle, and starts at around 48 K. This decrease of $\rho(T)$ across the transition is again associated with more and more of the sample being converted into a FM state. Within the hysteretic resistivity regime, the difference in resistivity values at any temperature is associated with the relative fraction of coexisting phases. [i.e., at any temperature within the hysteretic $\rho(T)$ regime, this fraction has a different value for the cooling and warming cycles.]

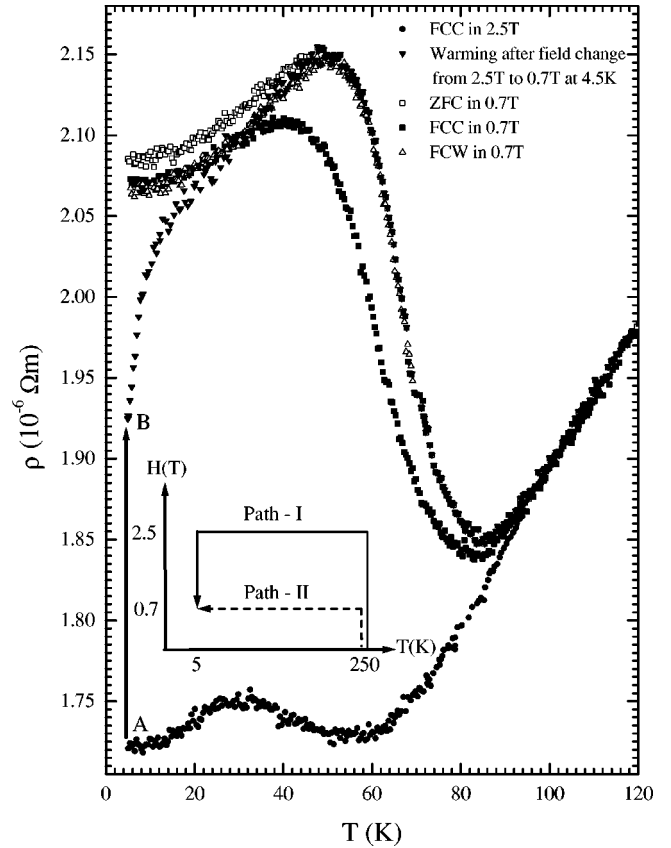


FIG. 5. The ρ vs T plot (filled down-triangle) for a $\text{Ce}(\text{Fe}_{0.96}\text{Al}_{0.04})_2$ sample recorded during a heating cycle initiated from a starting point (0.7 T, 4.5 K) represented as point B in the main panel following path I (shown in the inset). Path I involved two steps. While the first step (basically a FCC protocol in 2.5 T) is shown by filled circle symbols, the second step involving the isothermal field reduction from 2.5 T to 0.7 T, is shown by an arrow (from point A to point B in the main panel of the figure). For the purpose of comparison, the ρ vs T plots recorded for ZFC (open square symbols), FCC (filled square symbols), and FCW (open up-triangle symbols) protocols for $H=0.7$ T are also shown in the figure.

It is to be emphasized here that the transition from AFM-to-FM state during the warming cycle becomes complete at a distinctly higher temperature (≈ 93 K) than the onset of the FM-to-AFM transition (≈ 84 K) during a cooling cycle. Similar to this, the onset of the AFM-to-FM transition during a warming cycle takes place at a relatively higher temperature (i.e., ≈ 48 K) compared to the completion of the FM-to-AFM transition at ≈ 35 K during the cooling cycle. The difference in the two temperatures at both ends of the hysteretic regime is an indication that the FM-to-AFM transition in the present investigations of $\text{Ce}(\text{Fe}_{0.96}\text{Al}_{0.04})_2$ is first order in nature. As we shall see below, the effect of the applied field is to affect these various transition temperatures and the magnitude of thermal hysteresis in the resistivity (Fig. 2).

We wish to state here that the FM-to-AFM transition in the present case of a $\text{Ce}(\text{Fe}_{0.96}\text{Al}_{0.04})_2$ sample is quite broad on a temperature axis in comparison to the relatively sharp

FM-to-AFM transition observed in single-crystal manganese oxide perovskite samples.^{37–39} The broadening of a first-order transition with the disorder in the sample was predicted theoretically⁴⁰ in 1979, and very recently a magneto-optic imaging study on the vortex matter of a single-crystal Bi-2212 sample showed how the disorder leads to a distribution of transition temperatures and/or fields across the solid-to-liquid melting transition, which leads to heterogeneous nucleation across the transition.⁴¹ We believe that a similar distribution of transition temperatures and/or fields exists in the present case of a polycrystalline sample of $\text{Ce}(\text{Fe}_{0.96}\text{Al}_{0.04})_2$. Accordingly, the transition from one magnetic phase to another magnetic phase in the present work on $\text{Ce}(\text{Fe}_{0.96}\text{Al}_{0.04})_2$ should be designated here by a band, instead of a transition line on H - T phase space.

B. Minor hysteresis loops and phase coexistence

The study of minor hysteresis loops⁴² was recently recognized as an important experimental technique to study the phenomenon of phase coexistence across a FOT in more detail.^{33,35,43,44} Our magnetotransport results (Fig. 3) provide support in favor of phase coexistence across the foregoing AFM-to-FM transition. Consider the MHL's that were initiated well inside the hysteretic regime. They showed a strong irreversible behavior. For example, the MHL initiated on a cooling cycle at 60 K, during its course (i.e., while warming), did not come reversibly along the $\rho(T)$ of the cooling curve due to the already transformed AFM phase at 60 K. Instead, a slight increase in resistivity with T is observed along this initial course of the MHL due to the temperature dependence of transformed AFM phase, akin to the $\rho(T)$ behavior in the low-temperature AFM regime below 35 K. Upon further warming along the MHL, this increasing resistivity behavior changes back to a decreasing resistivity behavior due to more and more AFM-to-FM conversion, with the result that the MHL finally merges with the envelope warming cycle at about 70 K. The evidence of (a) phase coexistence and (b) the hysteresis due to the different fractions of FM and AFM phases is clearly obvious from the fact that the resistivity of the sample measured at any temperature, within the irreversible portion of a MHL, is drastically different than that recorded along either the envelope cooling or warming cycle at the same temperature.

On the other hand, the reversible behavior of a MHL, initiated from a warming cycle at 44.5 K (a temperature at which a distinct thermal hysteresis in resistivity exists between the envelope cooling and warming cycles), is due to the fact that the onset of nucleation of a FM state does not take place until 44.5 K during the warming cycle. Thus, while the sample is purely in an AFM state up to 44.5 K during the warming cycle, a finite fraction of the sample continues to remain ferromagnetic up to 35 K while cooling. With the same argument, the MHL initiated from the cooling cycle at 84 K, which took an overlapping course along the envelope cooling cycle, indicates the absence of any AFM phase at or above 84 K during the initial cooling cycle. This state of the sample (i.e., fully FM) at 84 K during the cooling cycle (as well as along the MHL under consideration) is in

sharp contrast to that along the envelope warming cycle, where the sample contains a finite fraction of an AFM phase (which is yet to transform into a FM state) even for $T > 84$ K, as indicated by the ρ vs T plot for $84 \text{ K} < T < 93 \text{ K}$ (Fig. 3). We note here that a clear coexistence of FM and AFM phases was also observed in zero-field neutron measurement¹² in a substantial T regime below the onset of the phase transition in $\text{Ce}(\text{Fe}_{1-x}\text{Al}_x)_2$ samples with $0.2 \leq x \leq 0.08$.

C. Metamagnetic transition and associated metastabilities

The ρ vs H plots for $T \geq 100$ K exhibited a typical ferromagnetic response, i.e., a negative magnetoresistance which increases in magnitude with field right from $H=0$. However, at lower temperatures, the ρ vs H plots in the virgin envelope as well as the field-increasing envelope cycle showed a field-induced AFM-to-FM transition, commonly referred to as a “metamagnetic transition,” resulting from spin flipping in the AFM phase at high enough fields.⁴⁵ The decrease of resistivity due to the onset of ferromagnetism at $H_m(T)$ continues (due to conversion of more and more of the antiferrophase into a ferrophase) until it reaches some higher field, after which the resistivity decreases linearly with the field, indicating the usual negative magnetoresistance ($\propto H$) behavior of the fully transformed high-field FM state of the entire sample. We note here that the positive magnetoresistance behavior (i.e., ρ increasing with an increase in H) of the AFM state is distinctly observed only in the low-temperature ρ vs H plot recorded at 2 K [Fig. 4(a)]. This positive sign of magnetoresistance in an AFM state is consistent with the previous reports⁴⁶ on Fe-Mn-Cr ternary alloys.

Along the H -decreasing envelope branch of a ρ vs H curve (for $T \leq 80$ K), the entire sample remains in the form of a high-field FM phase down to relatively lower-field values compared to those along either the virgin curve or the H -increasing envelope curve. This is expected across a first-order transition⁴⁷ as a sign of metastable behavior due to (a) a supercooling of the high-field FM phase below the transition field, and (b) a superheating of the low-field AFM phase above the transition field, when the field is cycled across a transition field (i.e., the H_m line or, more precisely, the H_m band). Further, one expects that for some value of H below $H_m(T)$ the resistivity behavior of the sample should once again become AFM-like. However, the results of Fig. 4(a) of this work and Fig. 2 of Ref. 36 clearly show that this is not the case with $\text{Ce}(\text{Fe}_{0.96}\text{Al}_{0.04})_2$. This is so because resistivity along the H -decreasing envelope curve is anomalous, since, on cycling the field back to $H=0$, the resistivity value corresponding to the low-field stable AFM phase [i.e., that of an H -increasing envelope curve (in the case of $T > 10$ K) and/or virgin curve (in the case of $T \leq 10$ K)] is not completely restored, with the result that an “open hysteresis loop” is obtained. A similar behavior was found in a virgin curve initiated in the negative H direction for $T \leq 10$ K (Ref. 36). This indicates that the FM phase persists in some finite quantity even at zero field after being cycled from $+H_{max}$ or $-H_{max}$. It is recalled here that although similar open hys-

teresis loops were also reported for $\text{Nd}_{0.5}\text{Sr}_{0.5}\text{MnO}_3$ (Ref. 37), the hysteresis loops in case of $\text{Pr}_{0.5}\text{Sr}_{0.5}\text{MnO}_3$ did not display any such open hysteresis loop (Ref. 38).

At lower temperatures, the anomalous open hysteresis loop in the $\rho(H)$ behavior is manifested in the form of another anomaly below 10 K, in that the virgin resistivity curve lies outside the butterfly-shaped (envelope) hysteresis loop [see, e.g., Fig. 4(a), the resistivity along the virgin $\rho(H)$ curve remains (up to H_m or so) distinctly above both the envelope H -increasing as well as H -decreasing ρ vs H curves]. In the case of magnetization measurements, this anomaly is observed in the form of a virgin $M(H)$ curve lying outside the butterfly (envelope) hysteresis loop.^{35,36} We come back to this anomalous result below H_m a little later. We are unaware of any such comparison based on the resistivity measurements in all three protocols (i.e., along the virgin curve, the field-increasing envelope curve, and the field-decreasing envelope curve) exists for either $\text{Nd}_{0.5}\text{Sr}_{0.5}\text{MnO}_3$, $\text{Nd}_{0.25}\text{Sm}_{0.25}\text{Sr}_{0.5}\text{MnO}_3$ and/or $\text{Pr}_{0.5}\text{Sr}_{0.5}\text{MnO}_3$ (Refs. 37–39).

D. Limits of metastability: Effect of magnetic field on the temperature dependence of the resistivity

It is important here to recall that there exists a limit of metastability^{47,48} below (above) the first-order transition line [in our case, the $H_m(T)$ or $T_N(H)$ line], up to which one can supercool (superheat) the high- (low-) field phase. Outside these two bounds [designated as $T^*(H)$ for supercooling and $T^{**}(H)$ for superheating] on either side of the transition line, no metastable behavior, and hence no superheating and/or supercooling, can be observed. [Recall that, like $T_N(H)$, as stated earlier, these two bounds $T^*(H)$ and $T^{**}(H)$ should be represented by the bands in the present case of a polycrystalline $\text{Ce}(\text{Fe}_{0.96}\text{Al}_{0.04})_2$ sample.]. It is also known that the metastable region widens with increase (decrease) of field (temperature). The natural question at this moment is the following: do we see such features of a FOT in the present $\rho(H, T)$ data of a $\text{Ce}(\text{Fe}_{0.96}\text{Al}_{0.04})_2$ sample?

The comparison of the resistivity behavior recorded on the $\text{Ce}(\text{Fe}_{0.96}\text{Al}_{0.04})_2$ sample under different protocols (ZFC, FCC, and FCW) has turned out to be very interesting, and displays almost all the above-mentioned generic features of a first-order phase transition. We find that the magnetic field has a very drastic effect on the $\rho(T)$ behavior, e.g., with increasing magnetic field.

(a) The completion of a FM-to-AFM transition while cooling the sample [which marks the lower limiting value of a $T^*(H)$ band, and is inferred by the temperature below which the FCC and FCW resistivities merge] is suppressed much faster than the decrease in the onset of an AFM-to-FM transition temperature while warming the sample [i.e., the upper limiting value of $T^{**}(H)$].

(b) The hysteretic regime is substantially enhanced in temperature across the transition.

(c) Most importantly, the low-temperature reversible $\rho(T)$ regime (with respect to the overlapping ZFC and FCC) disappears by $H \geq 0.7$ T.

Results (a) and (b) above clearly imply that with the increase in H , the lower limit of metastability, the $T^*(H)$ band

(below which one should see the reversible response of the stable AFM phase), is suppressed (toward lower temperature) even faster in comparison to the $T^{**}(H)$ band, and the metastable regime [existing between the lower limiting value of the $T^*(H)$ band and the upper limiting value of the $T^{**}(H)$ bands] thus widens with a decrease in T or with an increase in H . This is further supported from the isothermal ρ vs H data, where the hysteretic field regime drastically increased at low temperatures [Fig. 4(a)]. Based on T dependence of resistivity in different fields, a phase diagram using the midpoints of $T^*(H)$ and $T^{**}(H)$ bands was shown in our preliminary work.³⁶

Along the FCW curve, the resistivity rising past this merger point of FCW and FCC curves exhibits the superheating of the low-temperature AFM phase. The FCW curve finally merges with the ZFC curve at a temperature where the supercooled (metastable) FM phase formed during the FCC protocol vanishes. Above this field-dependent merger temperature of FCW and ZFC resistivities, the sample comprises of three fractions; (1) a stable transformed/nucleated FM phase, (2) a superheated metastable AFM phase, and (3) a stable AFM phase which has not yet transformed in a FM phase because of the distribution in the T_N 's in the sample.

It is now quite evident that the present study of $\rho(T)$ under different histories of applied magnetic field (i.e., ZFC, FCC, and FCW) in $\text{Ce}(\text{Fe}_{0.96}\text{Al}_{0.04})_2$ has an edge over previous work on $\text{Nd}_{0.5}\text{Sr}_{0.5}\text{MnO}_3$, $\text{Nd}_{0.25}\text{Sm}_{0.25}\text{Sr}_{0.5}\text{MnO}_3$ and/or $\text{Pr}_{0.5}\text{Sr}_{0.5}\text{MnO}_3$, where resistivity data were compared only during a FCC history with a FCW curve.^{37–39}

From the thermomagnetic irreversibility increasing with the field, as observed in the dc magnetization data of the same $\text{Ce}(\text{Fe}_{0.96}\text{Al}_{0.04})_2$ sample,^{35,36} it was argued that the hysteresis in the magnetization vs field was entirely due to the first-order nature of the magnetic transition rather than arising due to pinning of the domains formed in the FM state. All the results of the present magnetotransport study are in excellent agreement with those observed in dc magnetization studies.³⁵ This is so because, the hysteresis observed in the present bulk magnetotransport behavior cannot be related to the domain formation, since the domain size is normally much greater than the mean free path of the carriers.⁴⁶

E. Anomalous aspects of thermomagnetic history effects across the AFM-to-FM transition

We once again recall that in the case of a first-order transition, the free-energy barrier between the stable AFM phase and the metastable FM phase ceases to exist just below the $T^*(H)$ band, and any infinitesimal fluctuations can drive the entire sample to a stable AFM phase below the $T^*(H)$ line/band.⁴⁷ However, a few questions still remain unanswered in this picture.

(1) Why is the resistivity of the sample recorded in the FCC and FCW protocols not restored to that recorded in the ZFC protocol at lower temperatures (e.g., at 5 K) for $H \geq 0.7$ T? (We tend to believe that a similar feature would appear in the case of resistivity behavior in $\text{Nd}_{0.5}\text{Sr}_{0.5}\text{MnO}_3$ and $\text{Pr}_{0.5}\text{Sr}_{0.5}\text{MnO}_3$.) In our magnetization studies on the

same $\text{Ce}(\text{Fe}_{0.96}\text{Al}_{0.04})_2$ sample,^{35,36} this anomaly is reflected in the observation that the FC magnetization curve $M^{FC}(T)$ lie above the $M^{ZFC}(T)$.

(2) Why does the virgin ρ vs H curve lie outside the envelope butterfly $\rho(H)$ loop at lower temperatures, $T \leq 10$ K?

(3) Why is the full AFM resistivity not distinctly restored at $H=0$ on the envelope H -decreasing ρ vs H curve?

It once again should be remembered that the structural transition in a $\text{Ce}(\text{Fe}_{1-x}\text{Al}_x)_2$ system for $0.2 \leq x \leq 0.08$ from cubic to rhombohedral accompanies the AFM/FM transition.¹² We now argue that every structural transition is characterized by a characteristic relaxation time, which increases with decreasing temperature due to a reduction in the displacive motion of the atoms.⁴⁹ A typical example is the supercooled liquid-to-glass transition. It is our conjecture that in the present case of a $\text{Ce}(\text{Fe}_{0.96}\text{Al}_{0.04})_2$ sample, this characteristic relaxation time at low temperature may become much larger than the actual experimental time scale, with the result that kinetics of the transition is hindered. Within this picture, the anomalies enumerated above can be explained as follows. When the temperature is lowered, some high-temperature high-field metastable FM phase remains frozen in, resulting in the arrest of a FM-to-AFM transition at low temperature. In ρ vs H cycling, due to the low temperature, a finite amount of the supercooled FM phase continues to exist even when the applied field is reduced to zero. [Note that the magnetic field also induces the structural transition in $\text{Ce}(\text{Fe}_{0.96}\text{Al}_{0.04})_2$ (Ref. 4).] This metastable FM phase is then carried over when the direction of field is changed, and results in an H -decreasing (-increasing) envelope curve that lies below the virgin curve recorded in the negative (positive) H direction. As expected, such hysteresis loops are not seen at higher temperatures (> 10 K).

Another piece of evidence supporting the presence of hindered kinetics which, if not considered properly, might tempt one to draw false conclusions about the lower limit of metastable behavior, comes from the results of Fig. 5. As discussed above, the initial field cooling of the sample in a magnetic field of 2.5 T results in a finite fraction of a high-temperature FM phase existing at 4.5 K due to the hindered kinetics, as mentioned in preceding sections. Subsequent to this FC protocol, the isothermal (i.e., at 4.5 K) field reduction from 2.5 to 0.7 T yielded a resistivity value which is significantly smaller than either of $\rho(4.5 \text{ K}, 0.7 \text{ T}, \text{ZFC})$ and/or $\rho(4.5 \text{ K}, 0.7, \text{FCC/FCW})$, indicating that the metastable behavior in the sample existed at or below 4.5 K in a 0.7-T field. We believe this is due to the hindered kinetics because, while cooling the sample in 2.5 T a large fraction (compared to the 0.7-T FCC state at 4.5 K) of a supercooled high temperature FM phase is frozen, i.e., its transformation to a stable AFM phase at $T^*(H)$ is arrested. As a result, the resistivity of the sample at 4.5 K, after the field is reduced to 0.7 T, is significantly smaller than the FCC/FCW resistivity in 0.7 T at 4.5 K. On warming the sample, this anomalously low resistivity of the sample at 4.5 K increases quickly (as the sample gains energy in the warming process), and the resistivity merges at about 20 K with that of the kinetically hindered resistivity curve of 0.7 T. We thus assume that,

compared to field cooling in 0.7 T to 4.5 K (i.e., path II in the inset of Fig. 5), the kinetics of the FM-to-AFM transition experienced relatively more hindrance when the sample was field cooled to the same 4.5-K, 0.7-T point, but following path I.

It is to be noted here that results obtained following path-I experimental protocol (Fig. 5) are similar to the results of magnetic annealing effect reported in the Cr-doped manganese crystals of $\text{Nd}_{0.5}\text{Ca}_{0.5}\text{Mn}_{1-y}\text{Cr}_y\text{O}_3$ [see Fig. 2(b) of Ref. 50]. [We believe that the value of magnetization at 5 K in their sample at the annealing field of 7 T (which is not shown in Ref. 50)] would be much larger than the value obtained after field was reduced to 0.5 T at 5 K [see Fig. 2(b) of Ref. 50].) The authors of Ref. 50 explained their data on the basis of a random-field quenching due to Cr substitution, which produced FM microembryos. Our experimental results of magnetotransport studies (Fig. 5) are ascribed with an arrest of the first-order transition process at low temperature and high magnetic field. We further point out here that we have confirmed the magnetotransport results of Fig. 5 by a dc magnetization measurement (which is not shown here for the sake of conciseness) following similar path I as indicated in the inset of Fig. 5.

In Ref. 36, the hindrance to the kinetics of the transition was indicated on the H - T phase diagram through a (H_k, T_k) band (see Fig. 3 of Ref. 36). The reader is referred to Fig. 3(c) of Ref. 36 and the related text for a more illustrative understanding of hindered kinetics in the present case of $\text{Ce}(\text{Fe}_{0.96}\text{Al}_{0.04})_2$.

V. CONCLUSION

Magnetotransport behavior across the first-order phase transition from a low-field, low-temperature antiferromagnetic state to a high-field, high-temperature ferromagnetic state has been studied in a $\text{Ce}(\text{Fe}_{0.96}\text{Al}_{0.04})_2$ polycrystalline sample. This study on $\text{Ce}(\text{Fe}_{0.96}\text{Al}_{0.04})_2$ clearly demonstrated the various generic features of first-order phase transitions, viz., hysteresis, phase coexistence, field-dependent limits, and the existence of metastable supercooled and superheated phases across the transition boundary in a magnetic system. These results of our magnetotransport study not only support our previous dc magnetization study on the same sample, but also provide results extending to a relatively higher magnetic field and low temperature regime on the H - T phase space. We found some unusual magnetoresistance behavior (the most interesting one of which is the virgin resistivity curve lying outside the envelope resistivity loop) at lower temperatures. Based on the observed magnetotransport behavior using an unconventional history of application of magnetic field, we have ascribed the origin of these unusual features to the arrest of the transition at lower temperature.

ACKNOWLEDGMENTS

We thank R. K. Meena and Anil Chouhan for the assistance provided in the magnetotransport measurements.

- *Corresponding author, E-mail address: sujeetc@cat.ernet.in
- ¹D. F. Franceschini and S. F. Da Cunha, *J. Magn. Magn. Mater.* **52**, 280 (1985).
 - ²A. K. Rastogi and A. P. Murani, in *Theoretical and Experimental Aspects of Valence Fluctuations and Heavy Fermions*, edited by L. C. Gupta and S. K. Malik (Plenum, New York, 1987), p. 437.
 - ³S. B. Roy and B. R. Coles, *J. Phys. F: Met. Phys.* **17**, L215 (1987).
 - ⁴S. B. Roy, S. J. Kennedy, and B. R. Coles, *J. Phys. (Paris) Colloq.* **49**, C8-271 (1988).
 - ⁵A. K. Rastogi, G. Hilsher, E. Gratz, and N. Pillmayr, *J. Phys. (Paris) Colloq.* **49**, C8-277 (1988).
 - ⁶S. B. Roy and B. R. Coles, *J. Phys.: Condens. Matter* **1**, 419 (1989).
 - ⁷S. B. Roy and B. R. Coles, *Phys. Rev. B* **39**, 9360 (1989).
 - ⁸S. Radha, S. B. Roy, A. K. Nigam, and Girish Chandra, *Phys. Rev. B* **50**, 6866 (1994).
 - ⁹A. K. Rajarajan, S. B. Roy, and P. Chaddah, *Phys. Rev. B* **56**, 7808 (1997).
 - ¹⁰C. C. Tang, Y. X. Li, J. Du, G. H. Wu, and W. S. Zhan, *J. Phys.: Condens. Matter* **11**, 2027 (1999).
 - ¹¹H. Fukuda, H. Fujii, and H. Kamura, *Phys. Rev. B* **63**, 054405 (2001).
 - ¹²S. J. Kennedy and B. R. Coles, *J. Phys.: Condens. Matter* **2**, 1213 (1990).
 - ¹³S. J. Kennedy, P. J. Brown, and B. R. Coles, *J. Phys.: Condens. Matter* **5**, 5169 (1993).
 - ¹⁴L. Paolasini, P. Dervenagas, P. Vulliet, J.-P. Sanchez, G. H. Lander, A. Hiess, A. Panchula, and P. Canfield, *Phys. Rev. B* **58**, 12 117 (1998).
 - ¹⁵C. Giorgetti, S. Pizzini, E. Dartyge, A. Fontaine, F. Baudalet, C. Brouder, Ph. Bauer, G. Krill, S. Miraglia, D. Fruchart, and J.P. Kappler, *Phys. Rev. B* **48**, 12 732 (1993).
 - ¹⁶J. Ph. Schille, F. Bertran, M. Finazzi, Ch. Brouder, J. P. Kappler, and G. Krill, *Phys. Rev. B* **50**, 2985 (1994).
 - ¹⁷A. Delobbe, A.-M. Dias, M. Finazzi, L. Stichaure, J.-P. Kappler, and G. Krill, *Europhys. Lett.* **43**, 320 (1998).
 - ¹⁸R. J. Lange, I. R. Fisher, P. C. Canfield, V. P. Antropov, S. J. Lee, B. N. Harmon, and D. W. Lynch, *Phys. Rev. B* **62**, 7084 (2000).
 - ¹⁹J. Chaboy, C. Piquer, L. M. Garcia, F. Bartlome, H. Wada, H. Maruyama, and N. Kawamura, *Phys. Rev. B* **62**, 468 (2000).
 - ²⁰T. Konishi, K. Morikawa, K. Kobayashi, T. Mizokawa, A. Fujimori, K. Mamiya, F. Iga, H. Kawanaka, Y. Nishihara, A. Delin, and O. Ericksson, *Phys. Rev. B* **62**, 14 304 (2000).
 - ²¹M. J. Cooper, P. K. Lawson, M. A. G. Dixon, E. Zukowski, D. N. Timms, F. Itoh, H. Sakurai, H. Kawata, Y. Tanaka, and M. Ito, *Phys. Rev. B* **54**, 4068 (1996).
 - ²²H. Wada, T. Harada, and M. Shiga, *J. Phys.: Condens. Matter* **9**, 9347 (1997).
 - ²³H. P. Kunkel, X. Z. Zhou, P. A. Stampe, J. A. Cowen, and G. Williams, *Phys. Rev. B* **53**, 15 099 (1996).
 - ²⁴J. Deportes, D. Givord, and K. R. A. Ziebeck, *J. Appl. Phys.* **52**, 2074 (1981).
 - ²⁵S. Radha, S. B. Roy, and A. K. Nigam, *J. Appl. Phys.* **87**, 1 (2000).
 - ²⁶C. S. Garde, J. Ray, and G. Chandra, *Phys. Rev. B* **42**, 8643 (1990).
 - ²⁷E. Gratz, E. Bauer, H. Nowotny, A. T. Burkov, and M. V. Vedernikov, *Solid State Commun.* **69**, 1007 (1989).
 - ²⁸N. Ali and X. Zhang, *J. Phys.: Condens. Matter* **4**, L351 (1992).
 - ²⁹J. Eyon and N. Ali, *J. Appl. Phys.* **69**, 5063 (1991).
 - ³⁰X. Zhang and N. Ali, *J. Appl. Phys.* **75**, 7128 (1994).
 - ³¹D. Wang, H. P. Kunkel, and G. Williams, *Phys. Rev. B* **51**, 2872 (1995).
 - ³²R. Caciuffo, J.-C. Griveau, D. Kolberg, F. Wastin, D. Rinaldi, A. Panchula, and P. Canfield, *Phys. Rev. B* **85**, 6229 (1999).
 - ³³M. Manekar, S. B. Roy, and P. Chaddah, *J. Phys.: Condens. Matter* **12**, L409 (2000).
 - ³⁴M. Manekar, S. Chaudhary, M. K. Chattopadhyay, K. J. Singh, S. B. Roy, and P. Chaddah, *J. Phys.: Condens. Matter* **12**, 9645 (2000).
 - ³⁵M. Manekar, S. Chaudhary, M. K. Chattopadhyay, K. J. Singh, S. B. Roy, and P. Chaddah (unpublished).
 - ³⁶M. Manekar, S. Chaudhary, M. K. Chattopadhyay, K. J. Singh, S. B. Roy, and P. Chaddah, *Phys. Rev. B* **64**, 104416 (2001).
 - ³⁷H. Kuwahara, Y. Tomioka, A. Asamitsu, Y. Moritomo, and Y. Tokura, *Science* **270**, 961 (1995).
 - ³⁸Y. Tomioka, A. Asamitsu, Y. Moritomo, H. Kuwahara, and Y. Tokura, *Phys. Rev. Lett.* **74**, 5108 (1995).
 - ³⁹Y. Tokura, H. Kuwahara, Y. Moritomo, Y. Tomioka, and A. Asamitsu, *Phys. Rev. Lett.* **76**, 3184 (1996).
 - ⁴⁰Y. Imry and M. Wortis, *Phys. Rev. B* **19**, 3580 (1979).
 - ⁴¹A. Soibel, E. Zeldov, M. Rappaport, Y. Myasoedov, T. Tamegai, S. Ooi, M. Konczykowski, and V. B. Geshkenbein, *Nature (London)* **406**, 283 (2000).
 - ⁴²P. Chaddah, S. B. Roy, S. Kumar, and K. Bhagwat, *Phys. Rev. B* **46**, 11 737 (1992).
 - ⁴³S. B. Roy and P. Chaddah, *Physica C* **279**, 70 (1997).
 - ⁴⁴X. Granados, J. Fontcuberta, and X. Obradors, *Phys. Rev. B* **46**, 15 683 (1992).
 - ⁴⁵B.D. Cullity, in *Introduction to Magnetic Materials* (Addison-Wesley, Reading, MA, 1972), p. 240.
 - ⁴⁶T. K. Nath and A. K. Majumdar, *Phys. Rev. B* **57**, 10 655 (1998).
 - ⁴⁷P. M. Chaikin and T. C. Lubensky, in *Principles of Condensed Matter Physics* (Cambridge University Press, Cambridge, 1995).
 - ⁴⁸P. Chaddah and S. B. Roy, *Phys. Rev. B* **60**, 11 926 (1999).
 - ⁴⁹P. G. Debenedetti, in *Metastable Liquids* (Princeton University Press, Princeton, 1996).
 - ⁵⁰T. Kimura, Y. Tomioka, R. Kumai, Y. Okimoto, and Y. Tokura, *Phys. Rev. Lett.* **83**, 3940 (1999).